Two Tumor Suppressors, $p27^{Kip1}$ and Patched-1, Collaborate to Prevent Medulloblastoma

Olivier Ayrault,[1] Frederique Zindy,[1] Jerold Rehg,[2] Charles J. Sherr,[1,3] and Martine F. Roussel[1]

Departments of [1]Genetics and Tumor Cell Biology and [2]Pathology, and [3]Howard Hughes Medical Institute at St. Jude Children's Research Hospital, Memphis, Tennessee

Abstract

Two cyclin-dependent kinase inhibitors, $p18^{Ink4c}$ and $p27^{Kip1}$, are required for proper cerebellar development. Loss of either of these proteins conferred a proliferative advantage to granule neuron progenitors, although inactivation of *Kip1* exerted a greater effect. Mice heterozygous for *Patched-1* (*Ptc1+/–*) that are either heterozygous or nullizygous for *Kip1* developed medulloblastoma rapidly and with high penetrance. All tumors from *Ptc1+/–;Kip1+/–* or *Ptc1+/–;Kip1–/–* mice failed to express the wild-type *Ptc1* allele, consistent with its role as a canonical ''two-hit'' tumor suppressor. In contrast, expression of the wild-type $p27^{Kip1}$ protein was invariably maintained in medulloblastomas arising in *Ptc1+/–;Kip1+/–* mice, indicating that *Kip1* is haploinsufficient for tumor suppression. Although medulloblastomas occurring in *Ptc1+/–* mice were histopathologically heterogeneous and contained intermixed regions of both rapidly proliferating and nondividing more differentiated cells, tumors that also lacked *Kip1* were uniformly less differentiated, more highly proliferative, and invasive. Molecular analysis showed that the latter medulloblastomas exhibited constitutive activation of the Sonic hedgehog signaling pathway without loss of functional p53. Apart from gains or losses of single chromosomes, with gain of chromosome 6 being the most frequent, no other chromosomal anomalies were identified by spectral karyotyping, and half of the medulloblastomas so examined retained a normal karyotype. In this respect, this mouse medulloblastoma model recapitulates the vast majority of human medulloblastomas that do not sustain *TP53* mutations and are not aneuploid.

(Mol Cancer Res 2009;7(1):33–40)

Introduction

Normal cerebellar development requires the correct balance between the early proliferation of granule neuron progenitors (GNP) and their subsequent postmitotic differentiation and migration to their final location within the mature organ. In the mouse, GNPs arise in the rhombic lip during embryonic days E9.5 and E11.5 and migrate outward to form the external germinal layer (EGL) of the developing cerebellum (1). At birth (postnatal day 0; P0), the EGL is composed of a single layer of GNPs overlaying Purkinje cells that secrete the mitogen Sonic hedgehog (Shh). GNPs expressing the Shh receptor Patched-1 (Ptc1) are stimulated to undergo cell division, resulting in the rapid expansion of the EGL with maximum proliferation occurring at P5. GNPs then exit the cell cycle, differentiate, and migrate through the Purkinje cell layer to reside as postmitotic neurons within the internal granule layer (IGL). As they migrate, granule neurons extend retrograde axons that synapse with Purkinje neuron dendrites in the vacated EGL, thereby generating the outer molecular layer of the adult cerebellum, which is largely devoid of neuronal cell bodies. The cerebellum is completely formed within the first 3 to 4 weeks of life in the mouse and within 12 to 16 months in humans (1, 2).

Cell cycle progression of GNPs is regulated by the cyclin-dependent kinases, Cdk4 and Cdk6 that, in complexes with their allosteric regulators, cyclins D1 and D2, are required for proper development of the cerebellum (3). Opposing the action of cyclin-dependent kinases are two Cdk inhibitors, $p18^{Ink4c}$ and $p27^{Kip1}$, that enforce cell cycle exit and help to maintain the neuronal postmitotic state (4). Whereas $p18^{Ink4c}$ is a specific inhibitor of Cdk4 and Cdk6, $p27^{Kip1}$ preferentially targets cyclin E-dependent and cyclin A-dependent Cdk2, which acts later in G_1 phase to help guide the G_1 to S phase transition (5). *Ink4c* mRNA is transiently expressed just as proliferating GNPs in the EGL exit the cell division cycle and begin to migrate to the IGL (6). Although *Ink4c* mRNA expression is extinguished by P14, $p18^{Ink4c}$ is a stable protein that remains detectable throughout the migratory phase.[4] Unlike the transient expression of $p18^{Ink4c}$, $p27^{Kip1}$ expression is restricted to postmitotic neurons in the inner EGL and is maintained in granule neurons within the IGL throughout the life of the animal (6-8).

Received 8/5/08; revised 9/25/08; accepted 9/30/08.
Grant support: NCI grant P01-CA-096832 (M.F. Roussel and C.J. Sherr) an NCI Cancer Center Core grant CA-21765 to St. Jude Children's Research Hospital, La Fondation pour la Recherche Medicale and a Gephardt Endowed Fellowship (O. Ayrault), and the American Lebanese-Syrian Associated Charities of St. Jude Children's Research Hospital. C.J. Sherr is an Investigator of the Howard Hughes Medical Institute.
The costs of publication of this article were defrayed in part by the payment of page charges. This article must therefore be hereby marked *advertisement* in accordance with 18 U.S.C. Section 1734 solely to indicate this fact.
Note: O. Ayrault and F. Zindy contributed equally to this work.
Requests for reprints: Martine F. Roussel, Department of Genetics and Tumor Cell Biology, Mail Stop no. 350, 262 Danny Thomas Place, Memphis, TN 38105-3678. Phone: 901-595-3481; Fax: 901-595-2381. E-mail: martine.roussel@stjude.org

doi:10.1158/1541-7786.MCR-08-0369

[4] A. Forget, O. Ayrault, W. den BesFen, M-L. Kuo, C.J. Sherr, and M.F. Roussel, unpublished observations.

Medulloblastomas, the most common malignant pediatric brain tumors, are thought to arise, at least in part, from GNPs that fail to exit the cell cycle, migrate, and properly differentiate (9). Genetic anomalies in the SHH signaling pathway including mutations in *PATCHED* and *SUFU* (a negative regulator of the SHH-stimulated transcription factor GLI1) have been detected in ~25% of human medulloblastomas (1). Methylation of the *CDKN2C/INK4C* promoter was shown in ~10% of medulloblastomas from 43 patients admitted to St. Jude Children's Research Hospital, and a somewhat higher percentage (22% of 73 medulloblastomas) expressed no detectable $p18^{INK4C}$ protein (6). Although mice heterozygous for *Ptc1* develop medulloblastoma at a relatively low frequency (10-12), the time of onset and incidence of tumor development increases dramatically in an *Ink4c* nullizygous or heterozygous background (6). Low levels of $p27^{KIP1}$ have been associated with poor outcome in many forms of human cancer, including brain tumors such as astrocytoma and glioblastoma (13). However, the role of *Kip1* in medulloblastoma has not previously been evaluated. We now provide evidence that genetic disruption of either one or two alleles of *Kip1* in *Ptc1*+/– mice greatly increases the incidence of medulloblastomas. All such medulloblastomas lose expression of the wild-type *Ptc1* allele but retain functional p53, thereby providing a highly penetrant mouse medulloblastoma model that closely mimics a subset of the human disease (1).

Results

Expression of Cell Cycle Regulatory Proteins during Cerebellar Development

To compare the expression of key cell cycle regulators with that of $p27^{Kip1}$ and $p18^{Ink4c}$ during postnatal cerebellar development, we analyzed their protein levels in normal cerebellar tissues between P1 and P30 (Fig. 1A). Cyclin D1, cyclin D2, Cdk4, and Cdk2 protein levels peaked at P5, corresponding to the time of maximum GNP proliferation, and slowly decreased thereafter. Cdk2 levels were undetectable by P17, whereas cyclin D1, cyclin D2, and Cdk4 levels were maintained at low levels until P30. Cdk6 levels remained relatively constant between P1 and P20. $P27^{Kip1}$ was detected from P1 through P30; its level was relatively constant between P1 and P7 but increased at P10, as more cells exited the cell division cycle (6) and remained elevated thereafter. In contrast, $p18^{Ink4c}$ was barely detectable at P1. Its expression reached a peak at P10 after which it progressively declined and was no longer detectable by P20. Two other Cip/Kip proteins, $p21^{Cip1}$ and $p57^{Kip2}$, were not expressed at significant levels (data not shown), consistent with earlier reports (7, 8). Together, these data suggest that $p18^{Ink4c}$ and $p27^{Kip1}$ coordinate cell cycle exit, whereas the continuing expression of $p27^{Kip1}$ presumably helps to maintain neurons in their postmitotic state.

We next evaluated the effect of *Kip1* inactivation on the proliferation of cultured GNPs and compared the results with those obtained with GNPs lacking *Ink4c*, the loss of which was previously revealed to endow cells with an enhanced proliferative capacity (6). GNPs purified from the cerebella of wild-type, *Ink4c*-null, and *Kip1*-null mice were cultured in the absence of Shh for 1 day (Fig. 1B, a) or for 3 days (Fig. 1B, b), or in the complete absence of Shh for 1 day followed by a 2-day restimulation with Shh (Fig. 1B, c). Cultures were exposed to bromodeoxyuridine (BrdUrd) for 24 hours either throughout the duration of the 24-hour experiment (a) or during the final 24-hour intervals (b and c) before fixing the cells and determining the percentage that had incorporated the precursor. When deprived of Shh for 1 day, GNPs from *Kip1*-null, *Ink4c*-null, and wild-type mice displayed comparable levels of DNA synthesis with at least 30% of the cells incorporating BrdUrd during the labeling period (Fig. 1B, a). However, after 2 days of Shh starvation, virtually no GNPs from wild-type mice incorporated BrdUrd in the ensuing 24 hours; in contrast, a significant fraction of GNPs explanted from *Ink4c*-null and,

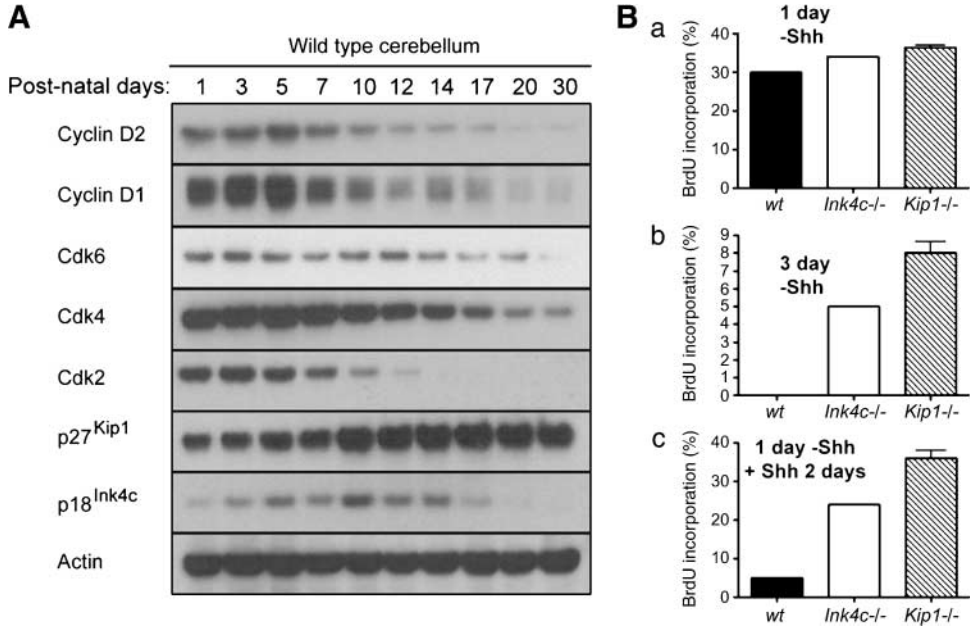

FIGURE 1. Expression of cell cycle regulators during cerebellar development. **A.** Expression of proteins (*left*) was detected by immunoblotting of protein lysates generated from the cerebella of postnatal (*P1-P30*) wild-type mice. Actin was used as a loading control. **B.** Columns, mean percentages of primary GNPs that incorporated BrdUrd under different culture conditions (**a**, **b**, and **c**). GNPs were purified from the cerebella of P10 mice of different genotypes [*black columns,* wild-type (*wt*); *unfilled columns, Ink4c*-null; and *shaded columns, Kip1*-null]. GNPs were cultured for 1 d (**a**) or 3 d (**b**) without Shh, or cultured 1 d without Shh followed by 2 d with Shh (**c**). BrdUrd was added 24 h before the fixation of cells.

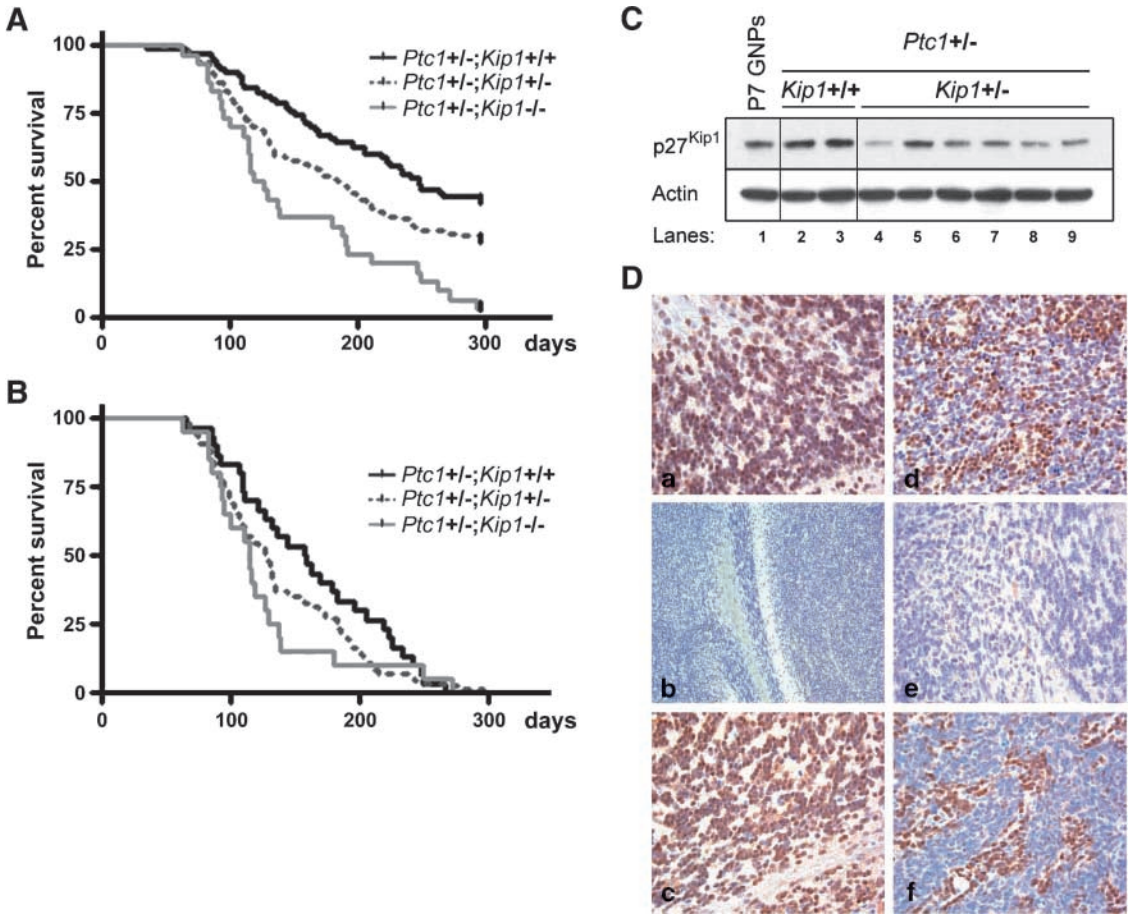

FIGURE 2. *Kip1* loss increases the incidence of medulloblastomas in *Ptc1* heterozygous mice. **A**. Illustration of survival curves for *Ptc1+/–* mice retaining two wild-type *Kip1* alleles (*+/+, black line*; $n = 70$), or lacking one (*+/–, gray dotted line*; $n = 144$) or two (*–/–, gray line*; $n = 30$) *Kip1* alleles. Mice showing signs of disease without any obvious brain tumors developed hydrocephaly, hemangiosarcomas, intestinal tumors, rhabdomyosarcomas, or lymphomas. Not all mice succumbed to tumors. **B.** Survival curves of *Ptc1+/–* mice of different *Kip1* genotypes with confirmed medulloblastoma development. Line designations are the same as for **A**; 30 mice in each cohort for *Kip1+/+*, 86 for *Kip1+/–*, and 20 for *Kip1–/–* genotypes. **C.** Detection by immunoblotting of the $p27^{Kip1}$ protein in GNPs purified from a P7 wild-type cerebellum and in purified tumor cells from medulloblastomas arising in *Ptc1+/–;Kip1+/+* and *Ptc1+/–;Kip1+/–* mice (*top*). Actin was used as a loading control. **D.** Expression of $p27^{Kip1}$ determined by immunohistochemistry (*brown*) in cerebellar sections from *Ptc1+/–* mice of different *Kip1* genotypes. All sections were counterstained with hematoxylin (*blue*). **a, b,** and **c,** sections taken from normal cerebellar tissues from *Ptc1+/–;Kip1+/+, Ptc1+/–;Kip1–/–*, and *Ptc1+/–;Kip1+/–* mice, respectively. **d, e,** and **f,** $p27^{Kip1}$ expression in medulloblastomas arising in *Kip1+/+, Kip1–/–*, and *Kip1+/–* mice, respectively. Magnification, ×10 (**b**) and ×40 (**a, c-f**). The unstained region represents the external molecular layer of the adult cerebellum which is practically devoid of cell bodies. **a** and **c,** cells within the $p27^{Kip1}$-positive IGL.

to a greater extent, *Kip1*-null mice could still incorporate BrdUrd (Fig. 1B, b). When GNPs were grown in the absence of Shh for 1 day followed by a 2-day restimulation with Shh, an even more significant proliferative advantage was documented for cells lacking either *Ink4c* or *Kip1* (Fig. 1B, c). These data are consistent with previous reports demonstrating enhanced *in vitro* proliferation of GNPs from *Kip1*-null mice compared with those from wild-type animals (7, 8). Therefore, loss of *Kip1* can delay cell cycle exit and maintain GNP proliferation even in the absence of Shh.

Increased Medulloblastoma Incidence in Ptc1+/–; Kip1+/– *and* Ptc1+/–;Kip1–/– *Mice*

To assess whether loss of *Kip1* might accelerate medulloblastoma formation in tumor-prone *Ptc1* heterozygous mice, *Kip1*-null mice were interbred with *Ptc1+/–* animals to derive *Ptc1+/–;Kip1+/–* offspring and later-generation *Ptc1+/–;Kip1–/–* cohorts that were prospectively followed for tumor formation. The overall survival of *Ptc1+/–* mice of the three possible *Kip1* genotypes revealed detrimental effects of *Kip1* loss of function on life span, with biallelic *Kip1* deletion exerting the most drastic effect (Fig. 2A). Although the majority of morbidity in these cohorts was due to medulloblastoma development, a fraction of the mice in each group developed other tumor types (hemangiosarcomas, intestinal tumors, rhabdomyosarcomas, and lymphomas) as well as hydrocephalus unrelated to tumor development (Table 1). The latter abnormalities collectively accounted for medulloblastoma-independent deaths as the animals were further aged (10, 12, 14).

Ptc1+/– mice were previously reported to develop medulloblastoma with a relatively low incidence (12-22%) and a mean time of tumor occurrence of 5 to 6 months (10, 12).

Table 1. The Incidence of Medulloblastomas and Other Tumors Arising in These Cohorts

Genotypes	Medullablastoma	Other tumors
Ptc1+/–;Kip1+/+	30/70 (42.8%)	10/70 (14.3%)
Ptc1+/–;Kip1+/–	86/144 (59.7%)	17/144 (11.8%)
Ptc1+/–;Kip1–/–	20/30 (66.7%)	9/30 (30%)

A greater incidence of medulloblastomas (42%) in *Ptc1+/–;Kip1+/+* mice from our colony (Fig. 2A) was most likely due to strain-specific genetic differences (14, 15). Loss of one or two alleles of *Kip1* further increased the overall incidence of medulloblastoma in *Ptc1+/–* mice to ~60% and ~67%, respectively (Table 1). Although the inactivation of one *Kip1* allele did not increase the incidence of other tumor types observed in *Ptc1+/–* mice (12-14% overall), 30% of *Ptc1+/–;Kip1–/–* mice developed tumors other than medulloblastomas (Table 1). No grossly overt pituitary tumors, a hallmark of *Kip1*-null mice (16-18), were observed in *Ptc1+/–;Kip1–/–* mice with medulloblastoma, reflecting the more rapid deaths of the compound-deficient animals. Indeed, when we limited our focus to those mice that developed medulloblastoma only (Fig. 2B), their median times of survival were shorter than those of their overall cohorts, documenting that medulloblastomas arose earlier than other tumor types (compare Fig. 2B to Fig. 2A). Among the animals with medulloblastoma only, the *Ptc1+/–;Kip1–/–* mice died somewhat more rapidly (median survival, 114 days) than the *Ptc1+/–;Kip1+/–* (127 days) or *Ptc1+/–;Kip1+/+* mice (158 days). Differences in survival between *Ptc1+/–;Kip1+/+* versus *Ptc1+/–;Kip1+/–* mice were not significant ($P = 0.13$), but inactivation of both *Kip1* alleles significantly accelerated medulloblastoma formation (*Ptc1+/–;Kip1+/+* versus *Ptc1+/–;Kip1–/–*; $P = 0.016$; *Ptc1+/–;Kip1+/–* versus *Ptc1+/–;Kip1–/–*; $P = 0.034$). Therefore, *Kip1* collaborates with *Ptc1* to prevent the development of medulloblastoma and other tumor types.

We confirmed by immunoblotting that $p27^{Kip1}$ expression was maintained in tumor cells purified from medulloblastomas resected from six of six *Ptc1+/–;Kip1+/–* mice (Fig. 2C, *lanes 4-9*). The levels of $p27^{Kip1}$ expressed in these tumors were approximately half of those detected in medulloblastomas arising in *Ptc1+/–;Kip1+/+* mice (Fig. 2C, *lanes 2* and *3*), consistent with the concept that *Kip1* is haploinsufficient for tumor suppression (19). Immunohistochemical staining of sections of normal cerebellar tissue from 1-month-old *Ptc1+/–* animals confirmed that $p27^{Kip1}$ was localized within the nuclei of mature postmitotic neurons residing in the IGL (Fig. 2D, a). As expected, no staining was detected in mature granule neurons in the IGL of *Ptc1+/–;Kip1–/–* mice (Fig. 2D, b), whereas $p27^{Kip1}$ was present in their *Kip1+/–* counterparts (Fig. 2D, c). $P27^{Kip1}$ was also found in the nuclei of medulloblastomas that arose spontaneously in *Ptc1+/–;Kip1+/+* mice (Fig. 2D, d), whereas as expected, it was not detected in medulloblastomas from *Ptc1+/–;Kip1–/–* mice (Fig. 2D, e). Notably, $p27^{Kip1}$ expression was retained in the nuclei of four of four *Ptc1+/–;Kip1+/–* medulloblastomas (Fig. 2D, f shows representative data). Because nucleotide sequencing of PCR-amplified *Kip1* cDNAs from the latter medulloblastomas revealed no mutations, the collective findings confirmed that *Kip1* is haploinsufficient for medulloblastoma suppression, as it is in other tumor types (19).

Medulloblastomas from Ptc1+/–;Kip1–/– *Mice Are Less Differentiated and More Invasive Than Medulloblastomas from* Ptc1+/–;Kip1+/+ *Animals*

Histologic examination of medulloblastomas revealed morphologic patterns that displayed distinctive immunohistochemical features, consistent with their degrees of cell differentiation (Fig. 3). Medulloblastomas from *Ptc1+/–;Kip1+/+* mice, although capable of expanding into large masses (Fig. 3A), were uniformly noninvasive (0 of 11). In 90% of cases, there was a biphasic architectural pattern (Fig. 3B) in which cells either expressed Ki-67, a marker of proliferation (Fig. 3C), or instead, the neuronal nuclear antigen (NeuN), a marker of differentiated neurons (Fig. 3D). However, focal regions of these tumors exhibited more anaplastic features in which virtually all cells were Ki-67–positive and NeuN-negative (data not shown). The histologic patterns in these murine tumors mimicked different phenotypes encountered in the human disease, including the classic biphasic phenotype and anaplastic variants seen in tumors with MYC amplification (20, 21).

In contrast, medulloblastomas from *Ptc1+/–;Kip1–/–* and *Ptc1+/–;Kip1+/–* animals were more invasive than medulloblastomas arising in *Ptc1+/–;Kip1+/+* animals and penetrated the white matter, in some cases, completely obliterating the normal contours of the cerebellar lobes (Fig. 3E). Uniform sheets of tumor cells (Fig. 3F) were mostly Ki-67–positive (Fig. 3G) and NeuN-negative (Fig. 3H). A similar frequency of invasion into the white matter was observed in 3 of 10 *Ptc1+/–;Kip1+/–* and 4 of 12 *Ptc1+/–;Kip1–/–* medulloblastomas, implying that invasiveness per se did not account for the accelerated demise of animals that were completely *Kip1*-deficient. Indeed, invasion was seen even more frequently in medulloblastomas arising in *Ptc1+/–;Ink4c–/–* mice (7 of 11; data not shown), although these animals have a better overall survival than *Ptc1+/–* mice lacking one or both *Kip1* alleles (6). Analysis of cerebella from 1-month-old *Ptc+/–;Kip1+/+*, *Ptc1+/–;Kip1+/–*, *Ptc1+/–;Kip1–/–* and *Ptc1+/–;Ink4c–/–* medulloblastoma–prone mice revealed preneoplastic lesions in the outer molecular layer where neuronal progenitors within the EGL had previously resided (data not shown); this suggests that medulloblastomas arose from GNPs within the EGL that failed to migrate. Thus, the increased morbidity of mice lacking *Kip1* alleles correlated most closely with the increased proliferative index of the tumor cells and their failure to differentiate.

Molecular Characterization of Medulloblastomas from Ptc1+/–;Kip1–/– *Mice*

Medulloblastomas from *Ptc1+/–* mice lose the expression of the wild-type *Ptc1* allele (22). We therefore assessed expression of *Ptc1* in purified tumor cells from medulloblastomas occurring in *Ptc1+/–;Kip1+/–* and *Ptc1+/–;Kip1–/–* mice. By quantitative real-time PCR, we found that *Ptc1* mRNA could not be detected in all such tumors (data not

shown), implying that the Shh signaling pathway was constitutively activated. To confirm this, tumor cells purified from the cerebella of *Ptc1+/–;Kip1–/–* animals were cultured in the presence of cyclopamine, a specific inhibitor of Shh signaling (23). These cells completely ceased proliferating after 3 days of treatment (data not shown), underscoring their dependence on the Shh pathway.

The transcription factor, Math1/Atoh1, is expressed in proliferating GNPs, but its expression is extinguished once GNPs in the EGL exit the cell cycle and begin to differentiate and start migrating toward the IGL (24). Down-regulation of Math1/Atoh1 in response to signaling by bone morphogenic proteins (BMP) or transcriptional repression mediated by Hic1 induces the neuronal differentiation of GNPs and of *Ptc1–/–* medulloblastoma tumor cells derived from them (25, 26), suggesting that Math1/Atoh1 expression is required to prevent the differentiation of GNPs. Math1/Atoh1 expression is also a hallmark of human medulloblastomas harboring a SHH signaling pathway expression signature (25). Immunoblotting of protein lysates revealed that Math1/Atoh1 was expressed in *Ptc1–/–* tumor cells purified from mice of all three *Kip1* genotypes (Fig. 4A), confirming that the Shh signaling pathway was constitutively activated in these medulloblastomas. The levels of Math1/Atoh1 were elevated in medulloblastomas from *Ptc1+/–;Kip1–/–* mice, consistent with the enhanced proliferative capacity and more aggressive nature of these tumors.

BMPs inhibit the proliferation of tumor cells from *Ptc1+/–;Ink4c–/–* mice and induce their differentiation by rapid posttranscriptional down-regulation of Math1/Atoh1 (25). Despite their relatively elevated levels of Math1/Atoh1 expression, tumor cells from *Ptc1+/–;Kip1–/–* mice remained sensitive to BMP treatment (S phase: 18% without treatment, 5% after BMP treatment; $n = 2$) suggesting that BMP-dependent cell cycle arrest and differentiation is independent of both *Kip1* and *Ink4c*.

$P21^{Cip1}$ and $p27^{Kip1}$ are necessary for the assembly and stability of D-type cyclins into complexes with Cdk4 and Cdk6 (5, 27). In turn, mouse embryo fibroblasts, hepatocytes, and thymic lymphoid cells lacking $p27^{Kip1}$ and $p21^{Cip1}$ each exhibited reduced levels of D-type cyclins (27). Although the levels of cyclin D1 in purified tumor cells from medulloblastomas from *Ptc1+/–;Kip1+/+* and *Ptc1+/–;Kip1+/–* mice differed between individual tumors, they were higher or equivalent to those observed in P7 wild-type GNPs (Fig. 4A). In the same tumors, cyclin D2 levels were somewhat less variable and were similar to those observed in P7 wild-type GNPs. However, reduced overall levels of cyclins D1 and D2 were observed in purified tumor cells from medulloblastomas arising in *Ptc1+/–;Kip1–/–* animals, consistent with previous observations that D-type cyclins are more rapidly degraded when $p27^{Kip1}$ is absent (27, 28). The fact that medulloblastomas lacking *Kip1* arise more rapidly implies that, in the absence of $p27^{Kip1}$, unfettered "downstream" Cdks drive the cell cycle even when cyclin D levels are reduced (28).

To assess their p53 status, tumor cells were purified from medulloblastomas of *Ptc1+/–;Kip1–/–* mice, cultured for 1 day, and then subjected to 15 Gy of ionizing radiation. P53 and $p21^{Cip1}$ protein levels, detected by immunoblotting 2 and 4 hours after irradiation, accumulated in response to ionizing radiation (Fig. 4B), confirming that p53 and a canonical p53-responsive gene product could be activated by DNA damage in these tumors. Spectral karyotyping analysis of medulloblastomas from *Ptc1+/–;Kip1+/–* and *Ptc1+/–;Kip1–/–* mice revealed that they had not sustained chromosomal translocations but exhibited recurrent gains of chromosomes 6 and 8 (Table 2). The most frequent event was trisomy 6 in 50% of cases (5 of 10), as previously reported in several mouse medulloblastoma models (29-31). The overall lack of aneuploidy and presence of a normal karyotype in half of the analyzed tumors is consistent with the fact that retention of p53 counters the widespread genomic instability generally associated with its loss of function.

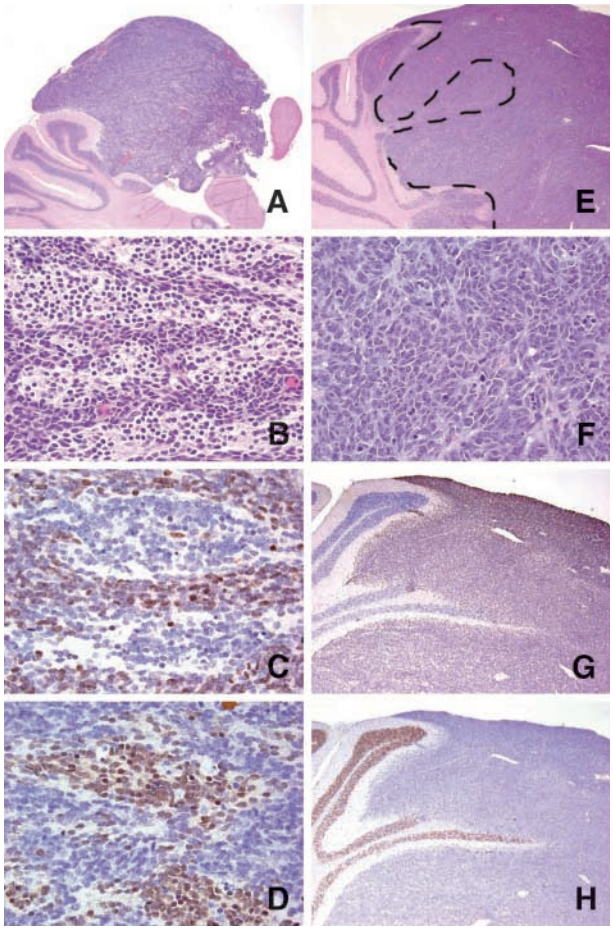

FIGURE 3. Pathologic characteristics of medulloblastomas. Tumors from *Ptc1+/–;Kip1+/+* mice (**A-D**) were noninvasive and confined to the periphery of the cerebellum (**A**), whereas those arising in *Ptc1+/–;Kip1–/–* mice (**E-H**) were more invasive and extended into the white matter (*interrupted black dashes,* contours of the invaded lobes; **E**). Sections were stained with H&E (**A, B, E,** and **F**) and by immunohistochemistry with antibodies to Ki-67 (**C** and **G**) or to NeuN (**D** and **H**) with a hematoxylin counterstain. Tumors that retained both *Kip1* alleles commonly exhibited a biphasic pattern (**B**) in which differentiated Ki-67–negative and NeuN-positive neurons were surrounded by proliferating Ki-67–positive and NeuN-negative cells (serial sections in **C** and **D**). *Kip1–/–* medulloblastomas were comprised of more uniform sheets of tumor cells (**F**) that were Ki-67–positive (**G**) and NeuN-negative (**H**). Magnifications, ×2 (**A**), ×40 (**B, C, D,** and **F**), and ×4 (**E, G,** and **H**).

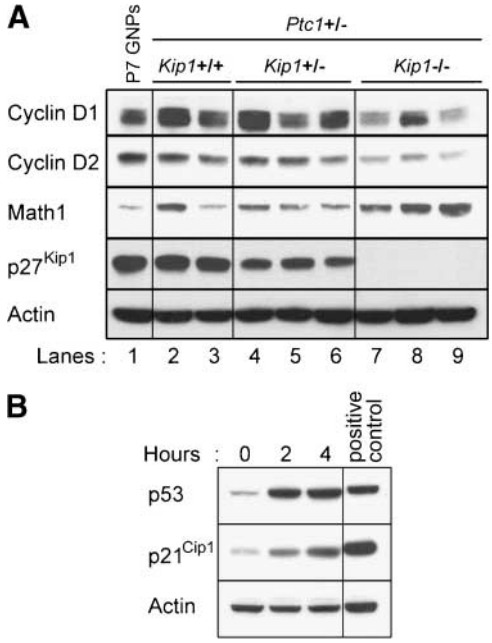

FIGURE 4. Molecular analysis of GNPs and medulloblastomas. **A.** Immunoblotting of the indicated proteins (*left*) expressed in primary GNPs purified from the cerebellum of a P7 wild-type mouse and from GNP-like tumor cells purified from medulloblastomas occurring in *Ptc1+/–* mice lacking no (+/+), one (+/–), or two (–/–) *Kip1* alleles. Actin was used as a loading control. **B.** Accumulation of p53 and $p21^{Cip1}$ 2 and 4 h after exposure to 15 Gy of ionizing radiation in tumor cells purified from medulloblastomas from *Ptc1+/–;Kip1–/–* mice. Zn^{2+}-treated MT-Arf cells were used as positive control.

Discussion

Several lines of evidence suggest that Ink4 and Cip/Kip1 proteins collaborate to induce G_1 phase arrest (5). In cycling cells, *Ink4* gene expression is limited, and most Cip/Kip proteins are assembled into complexes with cyclin D-Cdks. Induction of $p18^{Ink4c}$ and its binding to Cdk4 and Cdk6 not only disrupts cyclin D-Cdk complexes and accelerates cyclin D turnover but mobilizes $p27^{Kip1}$ into complexes with cyclin E/A-Cdk2, thereby inhibiting all G_1 cyclin-dependent kinase activity and inducing exit from the cell cycle. These interrelationships are consistent with observations that inactivation of either *Ink4c* or *Kip1* in mice leads to similar phenotypes, including organomegally and predisposition to certain tumor types (16-18, 32, 33). Moreover, both *Ink4c* and *Kip1* can act as haploinsufficient tumor suppressors (6, 19, 34). However, the fact that the simultaneous disruption of both genes widens the tumor spectrum and further accelerates tumor formation argues that the two Cdk inhibitors not only functionally collaborate but act synergistically (35).

The patterns of expression of $p27^{Kip1}$ and $p18^{Ink4c}$ during postnatal development of the cerebellum are consistent with their overlapping but differential functions in regulating cell cycle exit in GNPs. During the early postnatal period, the EGL rapidly expands, and maximal overall GNP proliferative rates are manifested at P5 to P7, after which the cells exit the division cycle and migrate into the IGL. $P27^{Kip1}$, which accumulated to maximal levels by P10, is detected exclusively in postmitotic GNPs, whether present in the inner part of the EGL during its expansion or later in the IGL; its expression in mature granule neurons then persists throughout the lifetime of the mice (6, 7). However, *Ink4c* mRNA expression in GNPs is transient, peaking at P7 but becoming undetectable by P14 (6). Because the $p18^{Ink4c}$ protein is relatively stable (half-life, ~12 hours),[4] its expression lags behind that of its mRNA. Peak levels of $p18^{Ink4c}$ were detected at P10 and declined slowly thereafter, vanishing by P17 to P20. Thus, $p18^{Ink4c}$ expression persists even in the absence of new synthesis throughout the period when most postmitotic cells migrate into the IGL.

Constitutive activation of the Shh signaling pathway induced medulloblastomas whose formation was accelerated when either one or two alleles of *Kip1* were co-inactivated. Although co-inactivation of *Ptc1* and *Kip1* alleles in the mouse germ line predisposed to several tumor types, medulloblastomas were by far the most frequent in the younger animals. Medulloblastomas from *Ptc1+/–;Kip1–/–* mice were less differentiated and more invasive than medulloblastomas from their *Ptc1+/–;Kip1+/+* counterparts, correlating with the greater incidence and more rapid course of medulloblastomas in animals lacking $p27^{Kip1}$ function. Medulloblastomas lacking *Kip1* expressed high levels of Math1/Atoh1, a basic helix-loop-helix transcription factor expressed exclusively in that subset of GNPs that are actively proliferating. This underscores the idea that $p27^{Kip1}$ helps to trigger the exit of GNPs from the cell cycle and enforces their differentiation. In tumors arising in *Ptc1+/–;Kip1+/–* mice, the wild-type $p27^{Kip1}$ protein was persistently expressed in purified tumor cells, consistent with previously documented *Kip1* haploinsufficiency in other tumor types (19). In contrast, the wild-type *Ptc1* allele was not expressed in tumor cells and functioned as a canonical tumor suppressor gene.

Although many mouse medulloblastoma models rely on the loss of functional p53 for high tumor penetrance, medulloblastomas from *Ptc1+/–;Kip1+/–* or *Ptc1+/–;Kip1–/–* mice, like those arising in *Ptc1+/–;Ink4c+/–* or *Ptc1+/–;Ink4c–/–* mice, retained functional wild-type p53 and were not aneuploid, similar to the vast majority of human medulloblastomas (1). This raises the possibility that inactivation of either *Kip1* or *Ink4c* might limit the p53 response to oncogenic signaling through the altered *Patched* pathway, thereby bypassing any

Table 2. Spectral Karyotyping of Medulloblastomas from Representative Tumors Arising in *Ptc1+/–;Kip1+/–* and *Ptc1+/–;Kip1–/–* Animals Was Used to Determine the Nature and Frequency of Chromosomal Anomalies

Mouse genotype	Tumor no.	Spectral karyotyping (no indicated events/no methaphases)
Ptc1+/–;Kip1+/–	63380	Normal
	62120	Normal
	62125	+6 (8/8)
	61080	+8 (14/14) +6 (2/14)
	64438	–X (3/12) +6 (5/12)
Ptc1+/–;Kip1–/–	62132	+6 (4/12) +8 (2/12)
	61786	+6 (4/9)
	63617	Normal
	63381	Normal
	64567	Normal

need to mutate p53 in this setting. Indeed, Carneiro and coworkers suggested that the absence of $p27^{Kip1}$ might curb the $p19^{Arf}$-induced p53 response during pituitary tumorigenesis (36); however, the inactivation of *Arf* does not accelerate medulloblastoma formation in *Ptc1+/−* mice (12), effectively ruling out such a mechanism. Neurons lacking *Ptc1* exhibit an increased sensitivity to DNA-damaging agents (37), so the retention of a functional p53 checkpoint in this subset of medulloblastomas implies that they would be more sensitive to genotoxic therapy than surrounding normal tissue.

Low levels of $p27^{KIP1}$ are associated with poor prognoses in many different human cancers, including brain tumors such as astrocytoma and glioblastoma (13, 38). Although the role of $p27^{Kip1}$ as a biomarker in human medulloblastoma remains unclear, determining its level of expression may have prognostic value, and its further evaluation in this disease is warranted.

Materials and Methods

Animal Husbandry

Kip1-null male mice (18) were bred to *Ptc1+/−* female mice (10) to obtain *Ptc1+/−;Kip1+/−* F1 animals. By intercrossing these double heterozygotes, we obtained *Ptc1+/+;Kip1+/−* females and *Ptc1+/−;Kip1+/−* males which were bred to one another to generate other genotypes. Mice were observed twice weekly for a period of 10 months. All mice were maintained on a mixed C57BL/6 × 129Sv background. The generation of *Ptc1+/−;Ink4c−/−* mice was previously described (6). Mice were housed in an American Association of Laboratory Animal Care–accredited facility and maintained in accordance with NIH guidelines. The Animal Care and Use Committee at St. Jude Children's Research Hospital approved all procedures. Survival curves and median survival were plotted and calculated using GraphPad Prism 4.

Purification and Culture of Primary GNPs and GNP-Like Tumor Cells

Purification of GNPs from the cerebella of mice with different genotypes and of GNP-like tumor cells from medulloblastomas were done as described (6, 25). Proliferation was determined by a BrdUrd incorporation assay done with 6×10^5 GNPs per milliliter plated in poly-D lysine and Matrigel precoated eight-well Lab-Tek glass dishes (6). We counted >500 cells per well and recorded the number of BrdUrd-positive cells detected by fluorescence within the total population enumerated by counterstaining with 4′,6-diamidino-2-phenylindole (Sigma). Each experiment was repeated at least thrice. Purified tumor cells were grown in the absence of Shh and treated with cyclopamine or BMP, as previously described (25). Zn^{2+}-inducible MT-Arf cells were used as positive controls for p53 and $p21^{Cip1}$ induction as previously described (39).

Protein Analysis by Immunoblotting and Quantitative Real-time PCR

Proteins extracted from cells were electrophoretically separated on polyacrylamide denaturing gels, transferred onto nitrocellulose membranes, and immunoblotted with the designated antibodies as previously described (30). Antibodies to mouse proteins used at 1:500 dilution were directed to cyclin D1 (72-13G), cyclin D2 (34B1-3), Cdk4 (C-22), Cdk6 (C-21), Cdk2 (M2), $p21^{Cip1}$ (F-5), and β-actin (C-11) (all from Santa Cruz Biotechnology); Math1/Atoh1 (Developmental Studies Hybridoma Bank, NIH); $p27^{Kip1}$ (clone 57; BD Transduction Laboratories); and p53 (1C12; Cell Signaling). Quantitative real-time PCR with RNA extracted from purified GNP-like tumor cells was done as described (30).

Histopathology, Immunohistochemistry, and Spectral Karyotyping

Histopathology and immunohistochemistry were done as previously described (30) using the following antibodies: anti-NeuN (clone A60, 1:50, Chemicon), anti-Ki67 (1:1,000; Vector Laboratories), and anti-$p27^{Kip1}$ (1:100, C19, Santa Cruz Biotechnology). Spectral karyotyping was done as previously described (30).

Disclosure of Potential Conflicts of Interest

No potential conflicts of interest were disclosed.

Acknowledgments

We thank all members of the Roussel/Sherr laboratory for helpful discussions. We also thank Robert Jenson, Shelly Wilkerson, and Deborah Yons for mouse husbandry, Suqing Xie for QRT-PCR; Robert Jenson, Suqing Xie, and Shelly Wilkerson for mouse genotyping; Shelly Wilkerson and Dorothy Bush for immunohistochemistry staining; Brenda McGowan and Shelly Wilkerson for tissue sectioning; Virginia Valentine for spectral karyotyping analysis; Rose Mathew for cultures of GNPs; and David Ellison for review of histopathology.

References

1. Marino S. Medulloblastoma: developmental mechanisms out of control. Trends Mol Med 2005;11:17–22.

2. Wang VY, Zoghbi HY. Genetic regulation of cerebellar development. Nat Rev Neurosci 2001;27:484–91.

3. Ciemerych MA, Kenney AM, Sicinska E, et al. Development of mice expressing a single D-type cyclin. Genes Dev 2002;16:3277–89.

4. Zindy F, Knoepfler PS, Xie S, Sherr CJ, Eisenman RN, Roussel MF. N-*Myc* and the cyclin-dependent kinase inhibitors $p18^{Ink4c}$ and $p27^{Kip1}$ coordinately regulate cerebellar development. Proc Natl Acad Sci U S A 2006;103:11579–83.

5. Sherr C, Roberts JM. CDK inhibitors: positive and negative regulators of G_1-phase progression. Genes Dev 1999;13:1501–12.

6. Uziel T, Zindy F, Xie S, et al. The tumor suppressors Ink4c and p53 collaborate independently with Patched to suppress medulloblastoma formation. Genes Dev 2005;19:2656–67.

7. Miyazawa K, Himi T, Garcia V, Yamagishi H, Sato S, Ishizaki Y. A role for p27/Kip1 in the control of cerebellar granule cell precursor proliferation. J Neurosci 2000;20:5756–63.

8. Ishizaki Y. Control of proliferation and differentiation of neural precursor cells: focusing on the developing cerebellum. J Pharmacol Sci 2006;101:183–8.

9. Gilbertson RJ, Ellison DW. The origins of medulloblastoma subtypes. Annu Rev Pathol Mech Dis 2008;3:341–65.

10. Goodrich LV, Milenkovic L, Higgins KM, Scott MP. Altered neural cell fates and medulloblastoma in mouse patched mutants. Science 1997;277:1109–13.

11. Goodrich LV, Scott MP. Hedgehog and patched in neural development and disease. Neuron 1998;21:1243–57.

12. Wetmore C, Eberhart DE, Curran T. Loss of *p53* but not *ARF* accelerates medulloblastoma in mice heterozygous for *patched*. Cancer Res 2001;61:513–6.

13. Chu IM, Hengst L, Slingerland JM. The Cdk inhibitor p27 in human cancer: prognostic potential and relevance to anticancer therapy. Nat Rev 2008;8:253–67.

14. Pazzaglia S. *Ptc1* heterozygous knockout mice as a model of multi-organ tumorigenesis. Cancer Lett 2006;234:124–34.

15. Pazzaglia S, Mancuso M, Tanori M, et al. Modulation of patched-associated

susceptibility to radiation induced tumorigenesis by genetic background. Cancer Res 2004;64:3798–806.

16. Nakayama K, Ishida N, Shirane M, et al. Mice lacking $p27^{Kip1}$ display increased body size, multiple organ hyperplasia, retinal dysplasia, and pituitary tumors. Cell 1996;85:707–20.

17. Kiyokawa H, Kineman RD, Manova-Todorova KO, et al. Enhanced growth of mice lacking the cyclin-dependent kinase inhibitor function of $p27^{Kip1}$. Cell 1996;85:721–32.

18. Fero ML, Rivkin M, Tasch M, et al. A syndrome of multiorgan hyperplasia with features of gigantism, tumorigenesis, and female sterility in $p27^{Kip1}$-deficient mice. Cell 1996;85:733–44.

19. Fero ML, Randel E, Gurley KE, Roberts JM, Kemp CJ. The murine gene $p27^{Kip1}$ is haplo-insufficient for tumour suppression. Nature 1998;396:177–80.

20. Ellison D. Classifying the medulloblastomas: insights from morphology and molecular genetics. Neuropathol Appl Neurobiol 2002;28:257–82.

21. McManamy CS, Pears J, Weston CL, et al. Nodule formation and desmoplasia in medulloblastomas—defining the nodular/desmoplastic variant and its biological behavior. Brain Pathol 2007;17:151–64.

22. Oliver TG, Read TA, Kessler JD, et al. Loss of patched and disruption of granule cell development in a pre-neoplastic stage of medulloblastoma. Development 2005;132:2425–39.

23. Berman DM, Karhadkar SS, Hallahan AR, et al. Medulloblastoma growth inhibition by hedgehog pathway blockade. Science 2002;297:1559–61.

24. Ben-Arie N, Bellen HJ, Armstrong DL, et al. Math1 is essential for genesis of cerebellar granule neurons. Nature 1997;390:169–72.

25. Zhao H, Ayrault O, Zindy F, Kim J-H, Roussel MF. Post-transcriptional down-regulation of Atoh1/Math1 by bone morphogenic proteins suppresses medulloblastoma development. Genes Dev 2008;22:722–7.

26. Briggs KJ, Corcoran-Schwartz IM, Zhang W, et al. Cooperation between the *Hic* and *Ptch1* tumor suppressors in medulloblastoma. Genes Dev 2008; 22:770–85.

27. Cheng M, Olivier P, Diehl JA, et al. The $p21^{Cip1}$ and $p27^{Kip1}$ CDK ''inhibitors'' are essential activators of cyclin D-dependent kinases in murine fibroblasts. EMBO J 1999;18:1571–83.

28. Geng Y, Yu Q, Sicinska E, Das M, Bronson RT, Sicinski P. Deletion of the $p27^{Kip1}$ gene restores normal development in cyclin D1-deficient mice. Proc Natl Acad Sci U S A 2001;98:194–9.

29. Yan CT, Kaushal D, Murphy M, et al. XRCC4 suppresses medulloblastomas with recurrent translocations in p53-deficient mice. Proc Natl Acad Sci U S A 2006;103:7378–83.

30. Zindy F, Uziel T, Ayrault O, et al. Genetic alterations in mouse medulloblastomas and generation of tumors *de novo* from primary cerebellar granule neuron precursors. Cancer Res 2007;67:2676–84.

31. Hatton BA, Villavicencio EH, Tsuchiya KD, et al. The Smo/Smo model: hedgehog-induced medulloblastoma with 90% incidence and leptomenigeal spread. Cancer Res 2008;68:1768–76.

32. Franklin DS, Godfrey VL, Lee H, et al. CDK inhibitors $p18^{INK4c}$ and $p27^{Kip1}$ mediate two separate pathways to collaboratively suppress pituitary tumorigenesis. Genes Dev 1998;12:2899–911.

33. Latres E, Malumbres M, Sotillo R, et al. Limited overlapping roles of $P15^{INK4b}$ and $P18^{INK4c}$ cell cycle inhibitors in proliferation and tumorigenesis. EMBO J 2000;19:3496–506.

34. Bai F, Pei XH, Godfrey VL, Xiong Y. Haploinsufficiency of $p18^{INK4c}$ sensitizes mice to carcinogen-induced tumorigenesis. Mol Cell Biol 2003;23: 1269–77.

35. Franklin DS, Godfrey VL, O'Brien DA, Deng C, Xiong Y. Functional collaboration between different cyclin-dependent kinase inhibitors suppresses tumor growth with distinct tissue specificity. Mol Cell Biol 2000;20:6147–58.

36. Carneiro C, Jiao MS, Hu M, et al. *p27* deficiency desensitizes *Rb*−/− cells to signals that trigger apoptosis during pituitary tumor development. Oncogene 2003;22:261–9.

37. Pazzaglia S, Mancuso M, Atkinson MJ, et al. High incidence of medulloblastoma following X-ray-irradiation of newborn Ptc1 heterozygous mice. Oncogene 2002;21:7580–4.

38. Slingerland J, Pagano M. Regulation of the cdk inhibitor p27 and its deregulation in cancer. J Cell Physiol 2002;183:10–7.

39. Kuo M-L, Duncavage EJ, Mathew R, et al. *Arf* induces p53-dependent and independent anti-proliferative genes. Cancer Res 2003;63:1046–53.